Electronic Supplementary Material (ESI) for Journal of Materials Chemistry A.

Supplementary Data

On the Effect of Anion Exchange Ionomer Binders in Bipolar Electrode Membrane Interface Water Electrolysis

Britta Mayerhöfer[a,b], Konrad Ehelebe[a,b], Florian D. Speck[a,b], Markus Bierling[a,b], Johannes Bender[c], Jochen A. Kerres[a,c,d], Karl J. J. Mayrhofer[a,b], Serhiy Cherevko[a], Retha Peach[a], Simon Thiele[a,b]

[a] *Forschungszentrum Jülich GmbH, Helmholtz-Institute Erlangen-Nürnberg for Renewable Energy (IEK-11), Egerlandstr. 3, 91058 Erlangen.*

[b] *Friedrich-Alexander University Erlangen-Nürnberg, Department for Chemical and Biological Engineering, Egerlandstr. 3, 91058 Erlangen.*

[c] *University of Stuttgart, Institute of Chemical Process Engineering (ICVT), Boeblinger Str. 78, 70199 Stuttgart.*

[d] *Focus Area: Chemical Resource Beneficiation Faculty of Natural Sciences, North-West University, Potchefstroom 2520, South Africa*

1. pH measurements

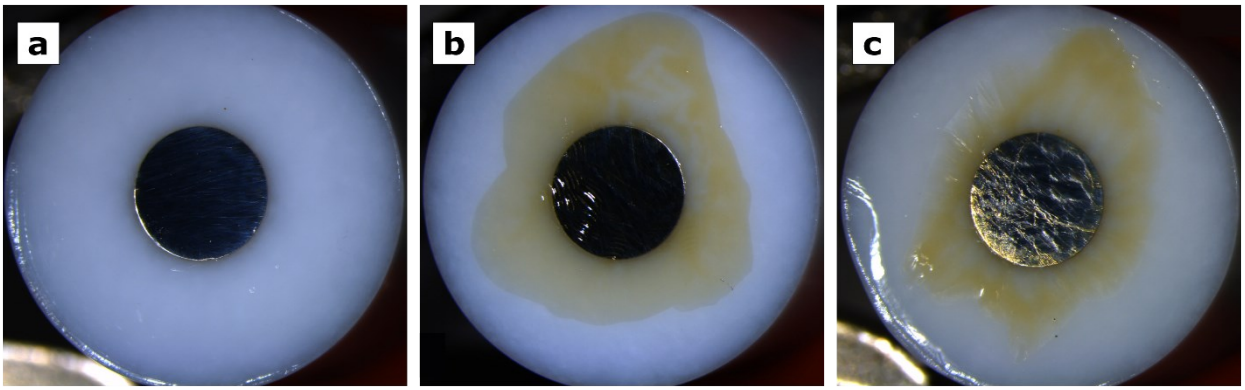

Figure S1 Polycrystalline Pt-RDE tips coated with 3-5 µm layer for local pH measurement. **a** Nafion cast from D520; **b** high IEC Aemion cast from a 5 wt% solution in 1-Propanol; **c** Nafion layer cast on top of a high IEC Aemion layer after polymer activation in 1 M KOH.

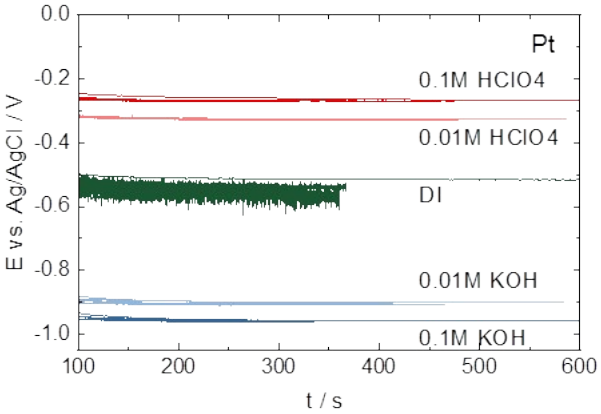

Figure S2 Overview on equilibration time of pure Pt-RDE disc without polymer layer in the respective electrolytes.

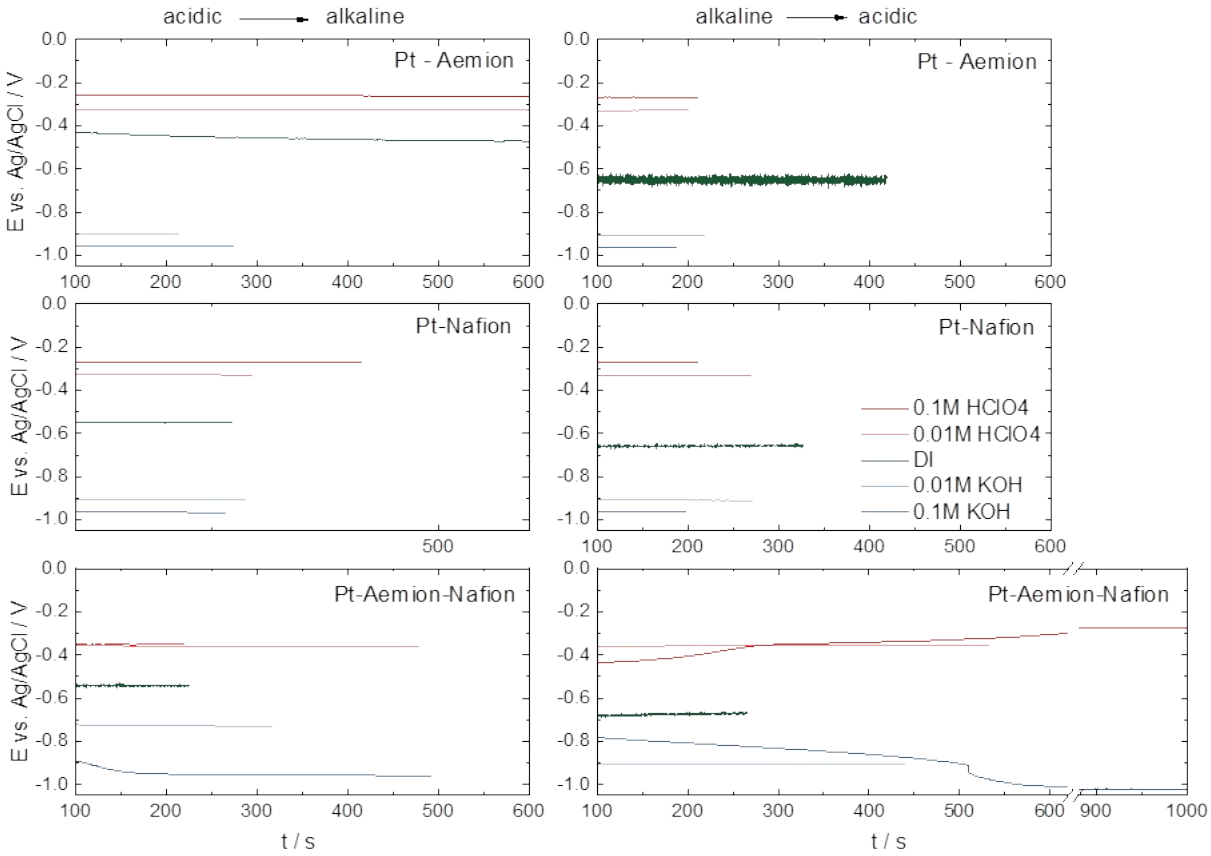

Figure S3 Overview on the RDE samples' equilibration time employing polymer films to cover the Pt-disc in respective electrolytes.

2. *Break-In behavior*

A sample with a Nafion 212 membrane was employed to prove the current density dependence of the break-in behavior of the BPEMWE cells. As Figure S4 suggests, the possibility of operating the system at higher current densities (due to a thinner Nafion membrane) results in a much faster break-in. Here, stable performance is already achieved after three polarization cycles, whereas roughly ten cycles were needed for the Nafion 115 membrane (Figure 7, main text).

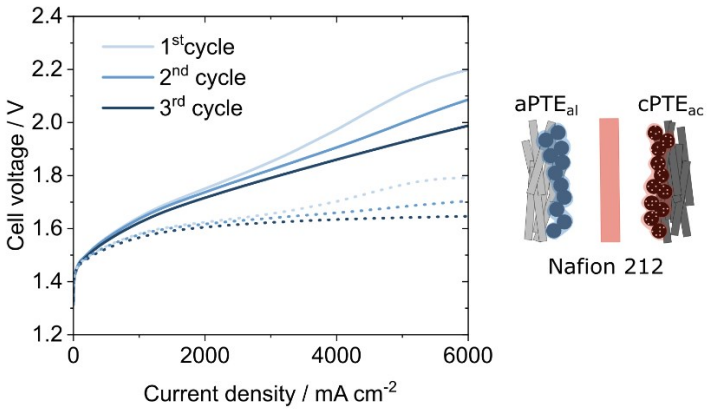

Figure S4 Break-In behavior of a BPEMWE MEA with a 50 µm thick Nafion 212 membrane and $aPTE_{al}$ containing 10 wt% high IEC Aemion binder in the catalyst layer. Performance remains stable after the first three polarization curves.

In a second control experiment, the cell was operated as described in the main text: After a constant voltage hold and the acquisition of polarization data at 50 °C, the operating temperature was ramped up to 80 °C. After another constant voltage hold, polarization data was acquired until the performance remained stable. Afterward, the operating temperature was lowered again to 50 °C without opening the cell, where further polarization curves were acquired. Both the electrolyte feed and the cathode compartment are purged with nitrogen during operation to exclude CO_2 from the ambient air to re-enter the catalyst layer in the form of carbonates. EIS analysis was conducted after every constant voltage hold at the respective temperatures and after performance stabilization at 80 °C.

Figure S5 features an overview of respective polarization data as well as electrochemical impedance (EIS) measurements at different stages during the test for 600 mA cm^{-2} attributed to the ohmic region and 1400 mA cm^{-2} or 2400 mA cm^{-2}, which is already part of the mass transport regime depending on the cell's condition. All EIS spectra were collected after a constant current hold time of two minutes employing a frequency range from 200 kHz to 0.1 Hz with 13 points per decade and an amplitude of 10 % of the direct current. No data fitting was employed. It has to be noted that the cell performance changed during the acquisition of the EIS data. Therefore, the Nyquist plots in Figure S5 can give some qualitative impressions on the changes in the MEA during break-in, particularly in the high current density regions. However, the quantitative analysis would not be meaningful.

As shown in Figure 7 in the main text, high-frequency resistance decreases throughout the cell's break-in, indicating decreasing ohmic resistance. We attribute this observation to improved hydroxide conductivity as carbonates from preconditioning are removed from the catalyst layer, particularly at high temperatures and high current densities. Moreover, the EIS spectra recorded for current densities in the mass transport regime, the arcs on the spectrum's low-frequency side are drastically enlarged compared to the ohmic region. After the break-in, this phenomenon is not observed anymore.

Figure S5b suggests that the large overpotentials at high current densities vanish irreversibly at high current density and high temperature operation. After performance stabilization at 80 °C, the HFR at an operating temperature of 50 °C is lower than in the initial measurements at 50 °C, and the mass transport associated overpotentials cannot be observed anymore.

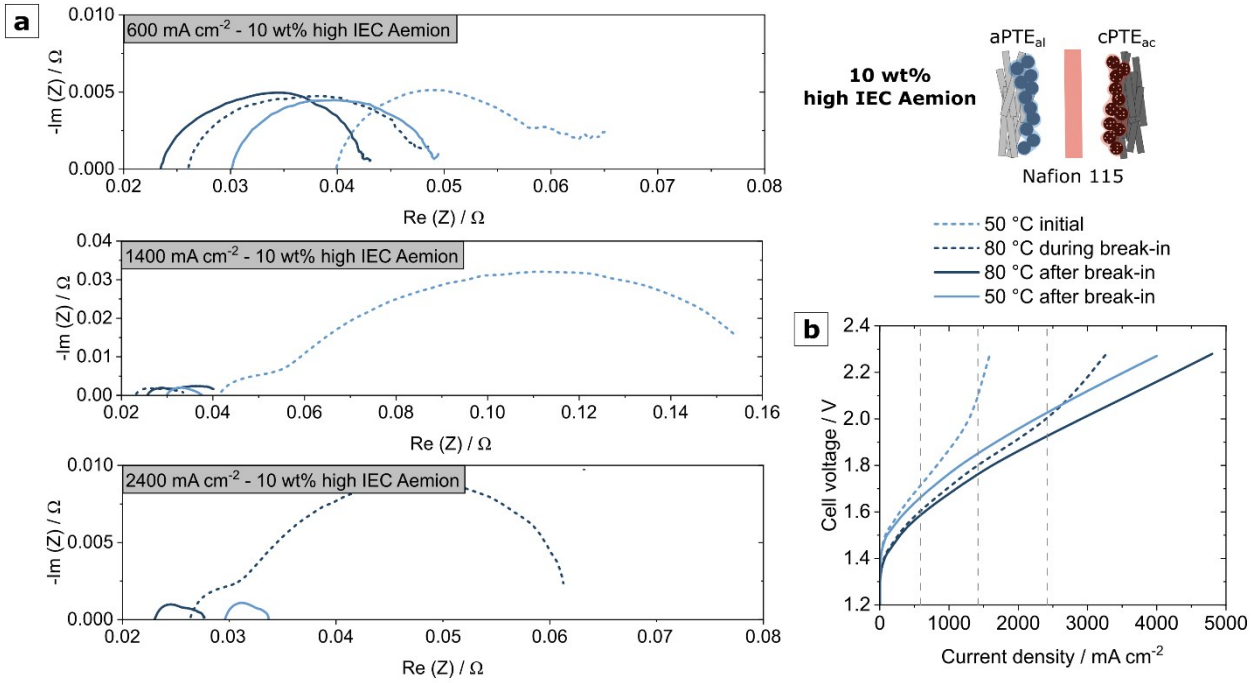

Figure S5 a Electrochemical impedance spectra collected at different stages of the cell's break-in exemplarily for the 10 wt% high IEC Aemion BPEMWE sample and **b** polarization curves at the respective stages of cell operation.

3. Water uptake

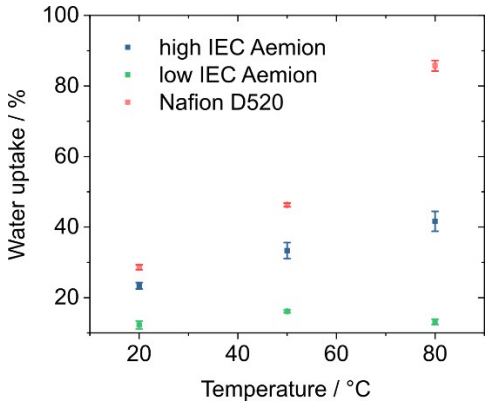

Figure S5 Temperature-dependent water uptake of ionomers used in this study.

For water uptake experiments, 1 cm² pieces of AF1-HNN8-25-X (high IEC Aemion) and AF1-HNN5-25-X (low IEC Aemion) were activated under the same conditions as stated in the main text. Nafion D520 was cast in a petri dish to yield a membrane with an approximate thickness of 20 µm. All samples were dried in a vacuum at 80 °C until their weight remained constant. The initial weight was determined using a microbalance (Cubis MSA66S, *Sartorius*). Samples were then immersed into ultrapure water at 20 °C, 50 °C, and 80 °C (three samples per polymer and temperature) for 10 h. The final weight was determined

after drying the membranes with a paper towel, and the water uptake was calculated from the difference between the initial and final weight.

4. Comparison to a non-conductive electrode binder and a commercial catalyst coated membrane

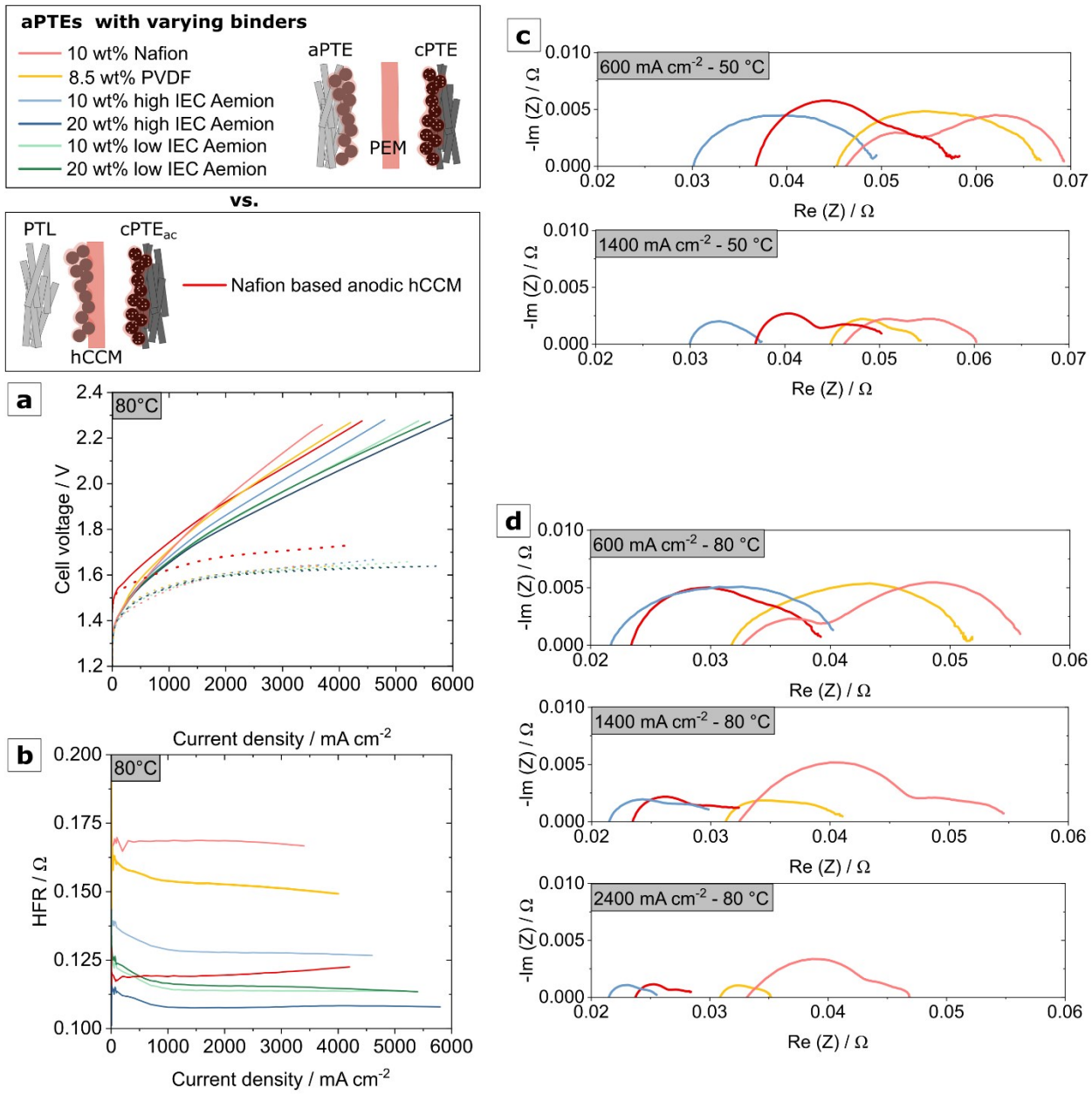

Figure S6 Comparison of different PTE-types employed in this study with an aPTE with PVDF as a non-conductive binder and an hCCM reference. **a** Polarization curves after performance stabilization. Dotted lines represent HFR-corrected data. **b** HFR data and **c** overview on EIS data of the PTE-based PEM reference with Nafion- and PVDF binder and the anodic hCCM and exemplarily the 10 wt% high IEC Aemion BPEMWE cell at 50 °C after performance stabilization (see also Figure S5) and **d** EIS data set at an operating temperature of 80 °C after performance stabilization, respectively.

To establish an idea of the Nafion binder's role in the PTE-based MEA approach, we additionally fabricated samples employing PVDF (Kynar HSV 900 polyvinylidene fluoride, *Arkema, Inc.*) as a non-conductive

electrode binder. Electrode fabrication was performed in the same fashion as described in the main text employing an ink with 1 wt% solids of which 2 wt% were PVDF. A 7:3 mixture of dimethyl formamide and acetone was employed as the ink solvent. The final ionomer content from TGA analysis was 8.5 wt%. A comparison of the surface structure to our Nafion aPTE reference sample is depicted Figure S7, reflecting a smoother surface of the PVDF sample compared to the Nafion-based PTE and the Aemion-based samples in this study. We attribute this to differences in the ink solvent's boiling point.

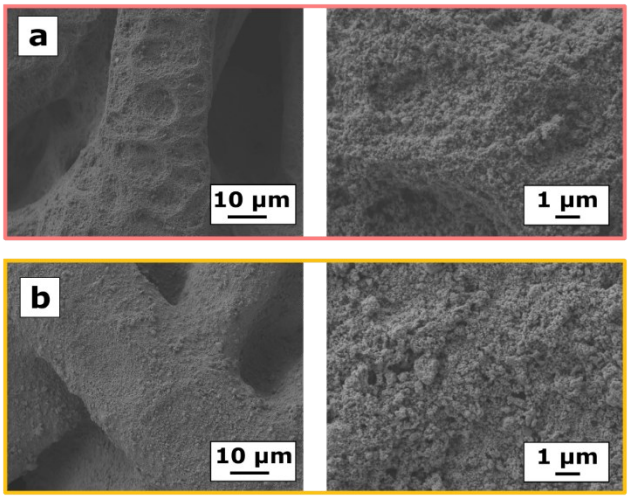

Figure S7 SEM micrograph of aPTE surface structure with **a** 10 wt% Nafion and **b** 8.5 wt% PVDF.

The PVDF-based aPTE sample's cell performance was in the same range but slightly better than that of the Nafion-based aPTE, which can be attributed to a slightly lower HFR (Figure S6b). However, the impedance data (Figures S6 c and d) points towards some additional contributions, which cannot be fully resolved at this stage. The influence of the anode electrode binder's proton conductivity seems to play a minor role in the PTE-based PEMWE system, which needs to be investigated in further studies on PEM water electrolysis.

Performance and HFR data of the BPEMWE cells were thus also compared to that of a commercial half sided catalyst coated membrane (hCCM, *FuelCellStore*) featuring an IrO_2 layer with 1.5 mg Ir loading coated onto the membrane for the anode. The cathode was the same type of gas diffusion electrode as employed in this study's other experiments (see MEA sketches in Figure S6). Also, the porous transport layer at the anode, the gaskets, and the resulting cell compression were the same. The exact ink formulation for the hCCM is a trade secret of the supplier. The higher onset-potential of the commercial cell compared to in-house fabricated MEA samples could be attributed to a different type of IrO_2 catalyst.

Nevertheless, the hCCMs performance exceeded that of the Nafion- and PVDF-based PTE setups, mainly an effect of drastically reduced ohmic resistance. Moreover, this experiment shows that the resistances in our optimized BPEMWE MEAs are very similar to what would be expected for an optimized catalyst coated membrane approach instead of the PTE-based setup (Figure S6a and b). A qualitative comparison of the EIS data for the hCCM reference and the BPEMWE cell at 80 °C (Figure S6d) shows a very similar Nyquist plot shape. At high current densities, the HFR represents the main difference between the two datasets.

This finding again highlights the possibility of drastically decreasing the HFR by employing the bipolar approach described in the main text. Thus, similar performances can be achieved for CCM- and PTE-based MEA setups.

5. Adhesion between Nafion and Aemion membranes

See supplementary video file